ELSEVIER

Engineering Structures 22 (2000) 180–190

ENGINEERING STRUCTURES

www.elsevier.com/locate/engstruct

Curved steel I-girder bridges: experimental and analytical studies

A. Zureick *, D. Linzell, R.T. Leon, J. Burrell

School of Civil and Environmental Engineering, Georgia Institute of Technology, Atlanta, GA 30332-0355, USA

Received 20 August 1997; accepted 9 January 1998

Abstract

This paper describes the large-scale experimental and analytical program, initiated by the Federal Highway Administration (FHWA), aimed at developing new rational design guidelines for horizontally curved steel bridges. Analytical and experimental efforts dedicated to establish the size of the full-scale components that will be tested as part of an entire three-girder bridge system are also presented. © 1999 Published by Elsevier Science Ltd. All rights reserved.

Keywords: Curved; Steel; Girder; Bridge; Testing; Design

1. Introduction

Due to the need to augment traffic capacity in urban highways and the constraints of existing land use, there has been a steady increase in the use of curved bridges in the past 25 years. In many cases these bridges are located in on- and off-ramps with very tight radii of curvature and are characterized by complex vertical and horizontal geometries. For this application, curved steel girders are the preferred choice because of the simplicity of fabrication and construction, speed of erection, and serviceability performance. Although horizontally curved steel bridges constitute roughly one-third of all steel bridges being erected today, their structural behavior is not well understood. To address this need, in 1992 the Federal Highway Administration (FHWA) initiated the Curved Steel Bridge Research Project (CSBRP), a large-scale experimental and analytical program aimed at developing new, rational design guidelines for this type of bridge. This on-going project is divided into six major tasks: synthesis of previous research, construction issues, determination of nominal bending and shear strength, connection details, serviceability considerations, and determination of the levels of analysis required for horizontally curved girders.

Presented in this paper are (a) a short discussion of past research and current research needs, (b) a description of the planned full-scale component tests and some early results, and (c) some results of the analytical study used to size the cross-frame components.

2. Previous research

Since 1843, when the first treatment of the analysis of curved beams was presented by Barré de Saint Venant [9], thousands of articles on the subject have appeared in the literature. However, serious studies pertaining to the analysis and design of horizontally curved bridges began only in 1969 when in the United States the FHWA formed the Consortium of University Research Teams (CURT). This team consisted of Carnegie Mellon University, The University of Pennsylvania, the University of Rhode Island, and Syracuse University, whose research efforts, along with those at the University of Maryland, resulted in the initial development of working stress design criteria and tentative design specifications. The American Society of Civil Engineers and the American Association of State Highway and Transportation Officials [5] compiled the results of most of the research efforts prior to 1976 and presented a set of recommendations pertaining to the design of curved I-girder bridges. The CURT research activity was followed by the development of Load Factor Design criteria [16,10] adopted by AASHTO [2–4] to go along with the working stress design criteria. These provisions appeared in

* Corresponding author. Tel.: + 1-404-894-2294; Fax: + 1-404-894-0211; E-mail: azureick@ce.gatech.edu

PII: S0141-0296(98)00107-2

the first Guide Specifications for Horizontally Curved Highway Bridges [2–4].

The first comprehensive bibliography on curved steel girders, containing over 200 references, was presented by McManus et al. [13]. Only four of these references dealt with box girders. McManus' paper was discussed by other authors who added additional references to the original list [12,15,17]. In 1978, the ASCE-AASHTO Committee on Flexural Members [6] presented another state-of-the-art report that contained 106 references dealing primarily with horizontally curved box girders. The Committee also presented results of a survey pertaining to the geometry, design, detail, construction and performance of box-girder bridges constructed in the United States, Canada, Europe, and Japan [7]. The survey was an update of a more limited survey published by the AASHO-ASCE Committee on Flexural members [1]. In 1988, Nakai and Yoo [14] published a book that offers a comprehensive listing of numerous modern papers, with particular attention paid to Japanese literature.

The first task of the CSBRP project was to produce a synthesis of the state-of-the-art in horizontally curved bridges. This led to the compilation of an up-to-date bibliography containing almost 900 references. A synopsis of the information contained in each of the references deemed most relevant was placed in an electronic database that is easy to access, query, and update as additional research is completed. A synthesis of the research into analytical methods commonly in use today indicated that [18]:

- The plane grid and space frame methods treat curved members as straight members, and hence are recommended only for preliminary design purposes. Similarly, the V-load method, which can be applied to I-girders only, underestimates innermost girder stresses, does not consider the bracing effect in the plane of the bottom flange, and its reliability depends on the selection of the proper live-load distribution factors. Thus, the V-load method can also only be recommended for preliminary analysis.
- Among the refined analytical methods (finite strip, finite difference, closed form solutions to differential equations and the slope-deflection method), the finite-element method is probably the most involved and time consuming. It is still the most general and comprehensive technique that has been applied to static/dynamic elastic/inelastic analysis with different mechanical and thermal loading. The other refined methods can be as good as the finite element method, but are limited to certain configurations and boundary conditions.
- Although a number of publications have addressed the geometrically and/or materially nonlinear behavior of horizontally curved bridges, the issue of when, why, and what level of inelastic analysis needs to be performed has not been resolved.

The following experimental research needs were identified with respect to behavior during construction and calculation of the ultimate strength of cross-sections [18]:

- Knowledge on stability issues related to curved box and I-girder bridges during construction is limited. The effects of ties, bracing, and web stiffeners on the distorsional behavior of these bridges during construction need to be studied, particularly with respect to box sections.
- A field experimental program to measure internal forces and deformations in the main girders and the bracing during construction is needed so that analytical models can be calibrated.
- Experiments demonstrating local and lateral-torsional buckling, both for composite and non-composite sections with different slenderness ratios are needed to clarify the validity of currently available methods. In the limit, a new set of theoretical solutions will need to be developed if it is found that existing methods do not provide for consistent reliability over the common range of design variables.
- Experiments demonstrating the limit states in a transversely and/or longitudinally stiffened web, including cases with spacing/depth ratios greater than 1, need to be conducted.
- Experiments addressing the effective width of the concrete slab in both curved I- and box girders need to be carried out.
- Cost-effective construction methods and erection guidelines that incorporate the experience of steel fabricators and erectors need to be developed.

In addition, the conclusions of this task reinforced the original objective of the CSBRP study, i.e. that a careful set of full-scale experiments was needed to clarify some of the more important fundamental issues related to both analysis and design of horizontally curved steel girder bridges.

3. Experimental design

To address a small portion of the research needs discussed above, a comprehensive series of tests was planned for the five remaining tasks in the CSBRP. The test series include specimens for determining the nominal strength in both bending and shear for non-composite I-girders. Curved box girders will be the subject of a future program if deemed necessary.

In the past, many of the laboratory tests on curved girders were conducted on either (a) full-scale girders with boundary conditions dissimilar from those encoun-

tered on a real bridge, and/or (b) small-scale specimens of real bridges where similitude could not be properly maintained for all relevant variables. Field investigations also have been performed [11]. Because of the shortcomings, as well as the lack of extensive material and geometrical data for several of these tests, most of the past experimental data cannot be used directly to calibrate analysis methods or design guidelines.

Based on this information, a key initial decision in the experimental design was that the test sections be part of a larger system that models an entire bridge rather than isolated specimens. In addition, because of the need to test at full-scale, the constraints of the available test space, and the desire to produce data that could be reliably utilized, a simply supported, rather than a continuous structure, was chosen. It was concluded that a minimum of three girders was needed to simulate the system behavior properly, but that only the central portion of the most heavily loaded girder (the outside girder) would be allowed to reach its full inelastic capacity.

The test frame "bridge" (Fig. 1) currently under construction at the FHWA Turner-Fairbank Research Center, consists of three concentric girders G1, G2, and G3 with radii of curvature 191.25 ft, 200 ft, and 208.75 ft, respectively (Fig. 1a). The center span of support girder G2 is 90 ft measured along its arc length. In the initial phase of the experimental program, I-girder component specimens B1 through B6 will be tested. Each of these components will have an arc length of 25.4 ft but with varying compression-flange and web-slenderness ratios, and will be spliced into the center of the outside girder (G3). The loading will be applied by jacks at roughly the third points of the span (Fig. 1b), and thus the test section will be subjected to nearly constant vertical bending moment.

Fig. 1 shows a three-dimensional (3-D) view of a finite element model of the test frame, which was used for the analytical studies. Table 1 shows the dimensions of the component specimens to be inserted in the middle portion of girder G3. Only this middle portion of girder G3 is intended to reach the inelastic range. The rest of the system has been designed to remain elastic and be reused for all tests. This represents a rational compromise between economy and the need to test a realistic 3-D model of the structure. Table 2 shows the sizes and nominal material properties for the main girders.

An important initial design decision was that the cross-frame members (Fig. 2) remain elastic so that they could be reused throughout the test series. Since the cross-frames are a key to the redistribution of forces in the structure, the use of typical cross-frame angle or T sections was ruled out because of the difficulty in interpreting experimental data. For this reason, pipe members were chosen. To minimize the differences in the load distribution in the elastic range as a result of using pipes instead of angle or T members, the pipes were designed to have both axial and bending stiffness and strengths similar to those encountered in practice.

A major analytical and experimental effort in the first part of this program was dedicated to establishing the sizes of the cross-frame members. Table 3 shows the final sizes for the cross-frame elements. Because of the need to maintain the cross-frames and girder G2, the most heavily loaded girder, in the elastic range, these components are being fabricated using high strength steel (70 ksi). The main result of these studies, a portion of which are discussed in detail within the following sections, was a resizing of the pipe thickness from the originally assumed 1/8 in. to the final 1/4 in.

As should be expected, careful thought and planning has gone into the development of the instrumentation and testing plans. The instrumentation will consist of approximately 800 data channels that include a mix of load cells, displacement transducers, inclinometers, and resistance and vibrating wire strain gages. Innovative techniques will be used to monitor both the forces at the supports, where all three components of force will be needed in order to properly check equilibrium, and the displacements of both the critical section of G3 and the main girders. For the former, it should be remembered that the spherical bearings which are being employed have a frictional component. Although small, usually in the range of 5% to 10% of the vertical force, these radial and tangential forces have a large impact on the overall equilibrium calculations and must be obtained in order to verify the integrity of the experimental data. Displacements will be measured, using both an elaborate system based on LVDTs and a state-of-the-art laser targeting system. The long-term performance of the frame, which is expected to be in use for about 2 years, will be monitored from the erection phase with the use of vibrating wire strain gages, which will ensure minimum long-term drift. Every effort has been made to incorporate independent checks on all key data channels.

4. Experimental determination of cross frame member forces

Before developing the experimental plan for the test bridge, considerable effort went into testing individual cross-frame members. This was done in order to determine their proportional limit and to optimize the number of strain gages necessary to monitor the forces in the cross-frame members. These forces are needed so that equilibrium of each girder, as well as of the whole system, can be ascertained. Each of the 21 cross-frames is made up of five individual elements, which in general are subjected to axial, bending, shear, and torsional forces. Since each cross-frame is a redundant structure, each element has to be instrumented. Taking advantage of the geometry of the pipe section, however, it can be

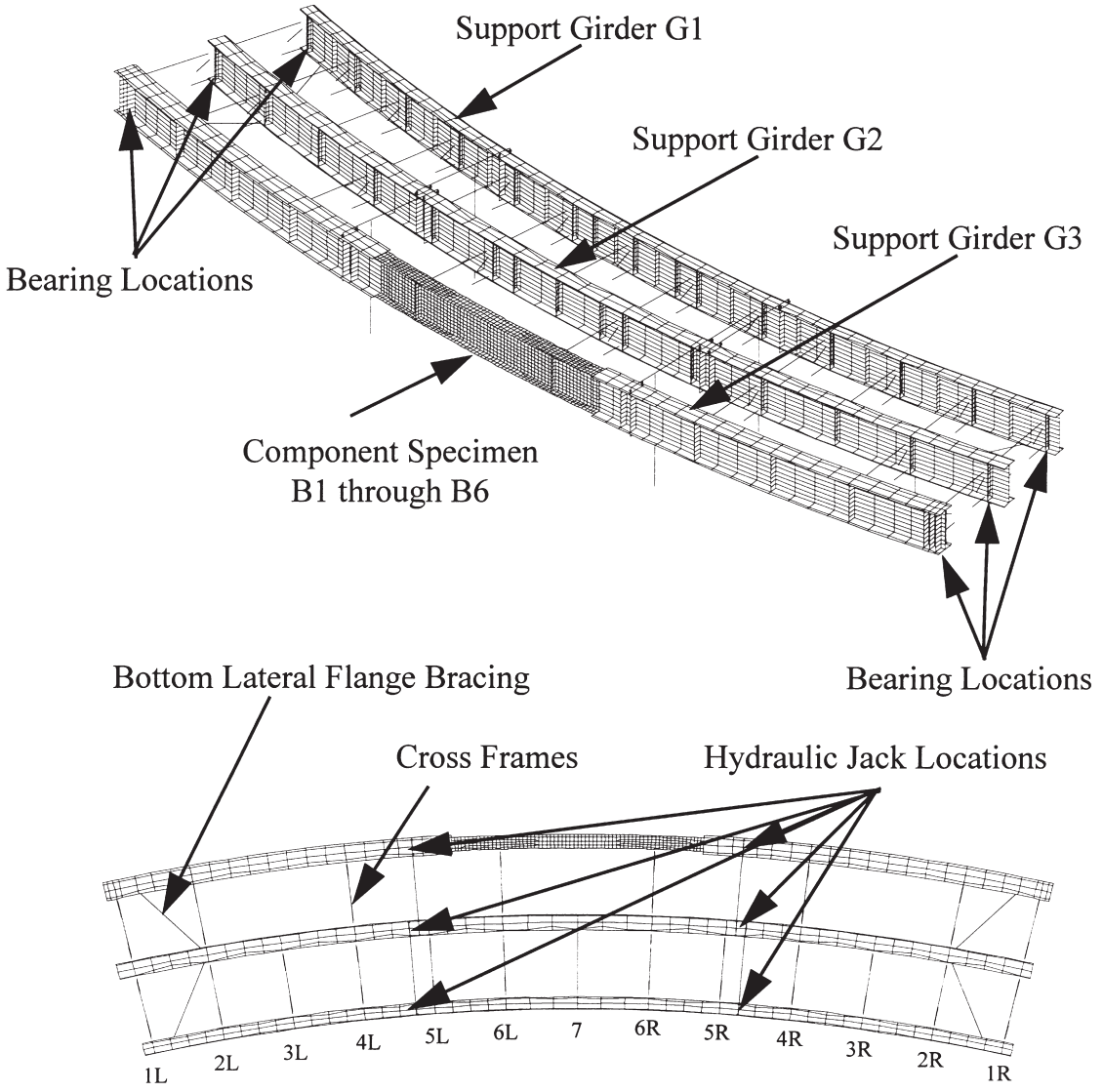

Fig. 1. Test configuration.

shown that four single-arm gages per member are sufficient to determine axial, shear and bending components. Although torsion occurs within the cross-frames, results from analytical studies of the curved bridge structure at hand indicated that the torsional effects would be small relative to axial, shear, and bending effects.

To determine the minimum number of strain gages required to measure the different force components, consider a tubular member occupying a region of three-dimensional space referred to a fixed Cartesian coordinate system in which the *x*- and *y*-axes lie in the plane of the cross-section while the *z*-axis coincides with the longitudinal axis of the tubular member (Fig. 3). Consider also the strain gage arrangement shown Fig. 3, where a total of eight single-arm and rosette gages are alternated every 45° around the tube's periphery. The rosettes are aligned so that their center arms are parallel to the specimen's longitudinal axis while single-arm gages were placed at alternating 0° and 45° angles along the longitudinal axis. The axial force, moments about the cross section's *x* and *y* axes, and torsional moment about the longitudinal axis (*z*-axis) can then be expressed in the forms:

$$P_A = \epsilon_{\text{avg}} AE \tag{1}$$

$$M_x = \frac{EI}{2r_o}(\epsilon_{\text{G2}} - \epsilon_{\text{G6}}) \tag{2}$$

$$M_y = \frac{EI}{(1-\nu)r_o}(\epsilon_{\text{G4}} - \epsilon_{\text{G8}}) \tag{3}$$

$$T_z = \frac{EJ}{4r_o(1-\nu)}[2(\epsilon_{\text{G4}} + \epsilon_{\text{G8}}) - (1-\nu)(\epsilon_{\text{G2}} + \epsilon_{\text{G6}})] \tag{4}$$

Table 1
Cross-sectional properties for test sections

Test	Flanges (in.)	Bottom flange (in.)	Web (in.)	Stiffeners (typical) (in.)	Diaphragm plates (in.)
B1	$\frac{3}{4} \times 17\frac{1}{2}$	$\frac{3}{4} \times 17\frac{1}{2}$	$\frac{5}{16} \times 48$	$\frac{7}{16} \times 5$ at 47 on center	$\frac{5}{8} \times 7$
B2	$\frac{3}{4} \times 17\frac{1}{2}$	$\frac{3}{4} \times 17\frac{1}{2}$	$\frac{3}{8} \times 48$	$\frac{7}{16} \times 5$ at 47 on center	$\frac{5}{8} \times 7$
B3	$\frac{3}{4} \times 17\frac{1}{2}$	$\frac{3}{4} \times 17\frac{1}{2}$	$\frac{3}{8} \times 48$	None	$\frac{5}{8} \times 7$
B4	$\frac{3}{4} \times 17\frac{1}{2}$	$1\frac{1}{4} \times 20$	$\frac{5}{16} \times 48$	$\frac{7}{16} \times 5$ at 47 on center	$\frac{5}{8} \times 7$
B5	$\frac{15}{16} \times 16\frac{7}{16}$	$\frac{15}{16} \times 16\frac{7}{16}$	$\frac{5}{16} \times 48$	$\frac{7}{16} \times 5$ at 47 on center	$\frac{5}{8} \times 7$
B6	$1\frac{3}{16} \times 16\frac{3}{16}$	$1\frac{3}{16} \times 16\frac{3}{16}$	$\frac{5}{16} \times 48$	$\frac{7}{16} \times 5$ at 47 on center	$\frac{5}{8} \times 7$

All dimensions in inches.

Table 2
Geometry and material properties for test specimen

Girder	Nominal yield stress F_y (ksi)	Top flange (in.)	Bottom flange (in.)	Web (in.)	Stiffeners (typical) (in.)
G1	50	$1\frac{1}{16} \times 16$	$1\frac{1}{16} \times 16$	$\frac{7}{16} \times 48$	$\frac{7}{16} \times 5$ at 44 on center
G2	70	$1\frac{3}{16} \times 20$	$1\frac{3}{16} \times 20$	$\frac{1}{2} \times 48$	$\frac{7}{16} \times 5$ at 48 on center
G3	50	$2\frac{1}{4} \times 24$	$2\frac{1}{4} \times 24$	$\frac{1}{2} \times 48$	$\frac{5}{8} \times 7$ at 51 on center

All dimensions in inches.

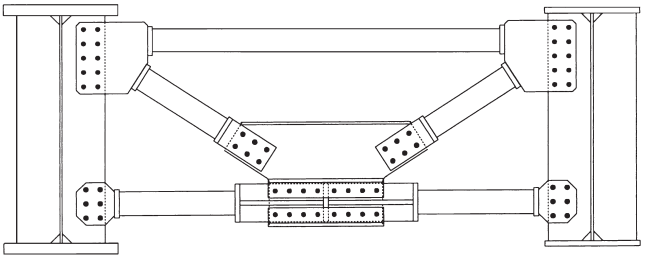

Fig. 2. Typical cross-frame configuration.

where P is the axial force, M_x and M_y are the moments about the x and y axes, respectively, A is the area, I is the moment of inertia, r is the radius of gyration, J is the torsional constant, E is Young's modulus, ν is Poisson' ratio, ϵ_{avg} is the average longitudinal strain for opposite gage pair, and the $\epsilon_{Gi}(i = 2, 4, 6, 8)$ are the strains corresponding to gages 2, 4, 6, and 8 as shown in Fig. 3. If more accuracy is desired for the axial load and torsional and shear forces are small or not important, it is also possible to derive the axial forces and moments directly from four longitudinal gages.

To confirm the above mathematical calculations experimentally, full-scale replicas of the upper cross-frame member, shown in Fig. 4, were tested concentrically in tension, concentrically in compression, and eccentrically in both tension and compression. The eccentric tests included cases in which single and double curvature moment gradients were induced. Shorter members, representing the diagonals and bottom chords, were later tested. In each test, four three-element strain gage rosettes and four single-element strain gages were mounted at the mid-height of the tubular member with the orientation shown in Fig. 3. A load cell was used to monitor the applied load. For brevity, only set-up and results of the concentric tests are presented hereafter.

Table 3
Cross-frame members

Diaphragm component	Length (in.)	Diameter (in.)	Thickness (in.)	Minimum yield stress (ksi)
Top member	$76\frac{1}{2}$	5	$\frac{1}{4}$	70
Bottom member	$27\frac{1}{4}$	5	$\frac{1}{4}$	70
Diagonal member	$22\frac{5}{8}$	5	$\frac{1}{4}$	70

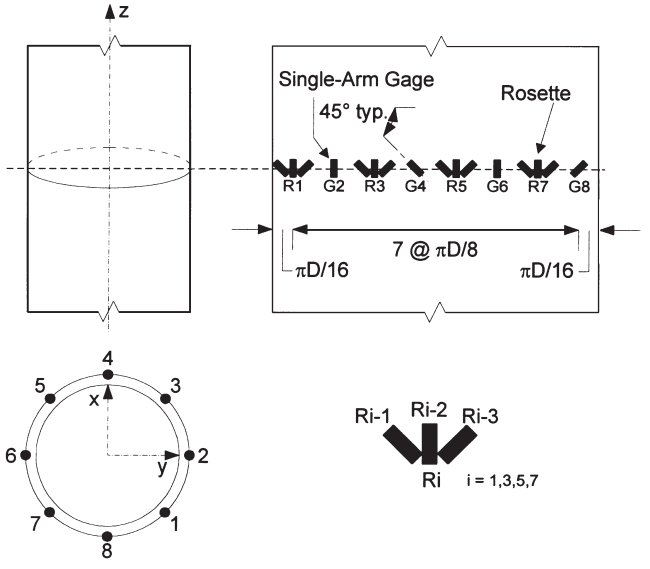

Fig. 3. Mid-height strain gage detail.

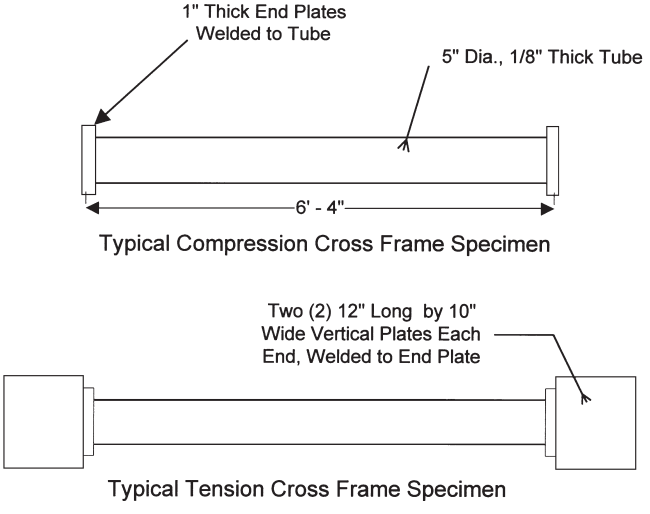

Fig. 4. Typical cross-frame specimen schematics.

5. Concentric cross-frame specimen tests

Four cross frame specimens, designated as 1C, 2C, 3C, and 6C, were tested under concentric compressive load and one specimen, 1T, was tested under concentric tensile load. Wall thickness for specimens 1C through 3C was 1/8″, and for specimens 6C and 1T was 1/4″. All specimens, except 3C, were fabricated using groove welds to connect the end plates to the pipe (Fig. 3). Specimen 3C utilized fillet welds and results from its test were compared to those for 2C to investigate the effects of fabrication changes on the member capacity. Specimen 1C was tested to establish an initial member capacity and to validate the data reduction system. Therefore, the specimen was placed directly into the testing machine with no load transfer or support mechanisms and loaded past its yield point. A schematic of this configuration is shown in Fig. 5.

Tests on specimens 2C and 3C were carried out not only to check the accuracy and robustness of the data reduction algorithms, but also to examine the effects of the fabrication method on capacity. Since direct comparisons were going to be made, pinned-pinned simu-

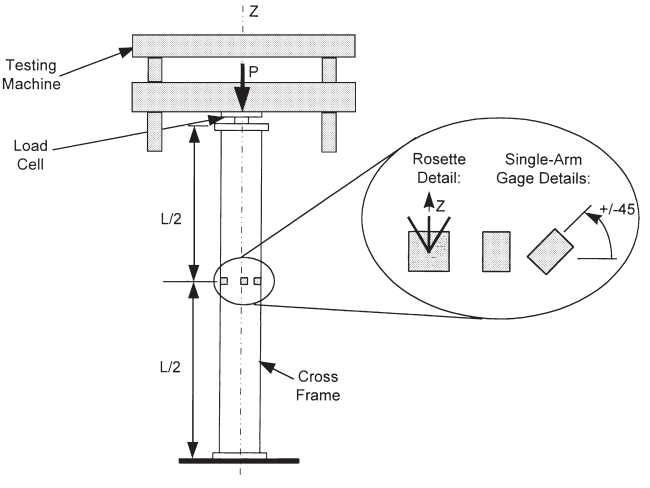

Fig. 5. Elevation of concentric compression, Test 1C.

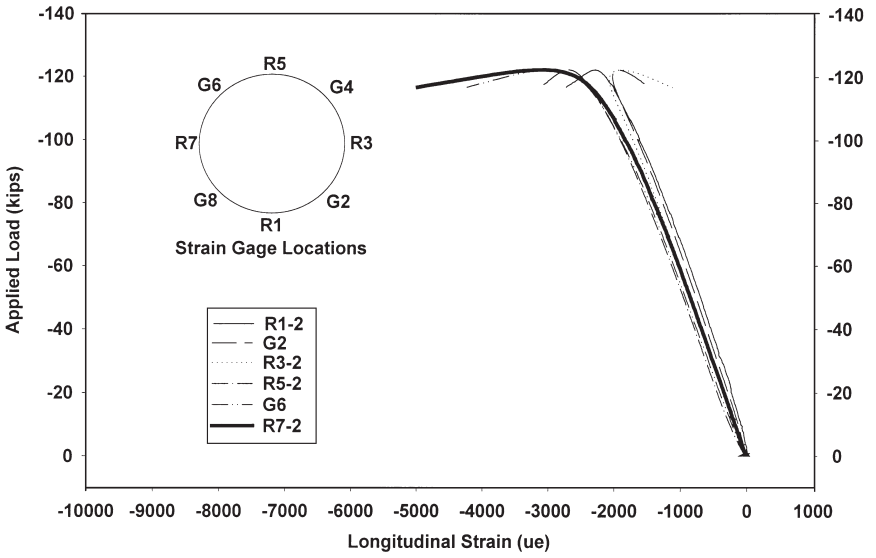

Fig. 6. Results of compression tests on concentrically loaded cross-frame pipe component.

lated end conditions, using knife edges top and bottom, were utilized. The carefully constructed knife edges, made of hardened steel, facilitated alignment, improved repeatability of test results, and allowed accurate comparisons to be made. Specimen 6C, which was tested in a similar configuration to specimens 2C and 3C, was utilized to check capacity increases resulting from doubling the wall thickness.

A complete overhaul of the testing configuration was required for the concentric tension test conducted on specimen 1T. Pins were inserted through vertical plates welded to the ends of the 1/4″ thick specimen (Fig. 4). These pins were then connected to additional steel plates, which were either gripped by or bolted to the testing machine.

The eight alternating single-arm gages and rosettes were placed at 45° intervals around each tube's periphery at mid-height. Rosettes were aligned so that their center arms fell on the longitudinal axis (z-axis) of each specimen, while single-arm gages were placed at alternating 0° and 45° angles with respect to this axis, as shown in Fig. 4. For all specimens except 1C, the mid-height deflection, and loaded end axial deformation and rotation were measured using LVDTs, potentiometers and inclinometers.

Each specimen was placed into the testing machine and a pre-load ranging from 1 to 2 kips was applied to keep the system stable. After stability was achieved and all instrumentation was checked, the specimen was loaded at a constant rate of approximately 10 kips/min

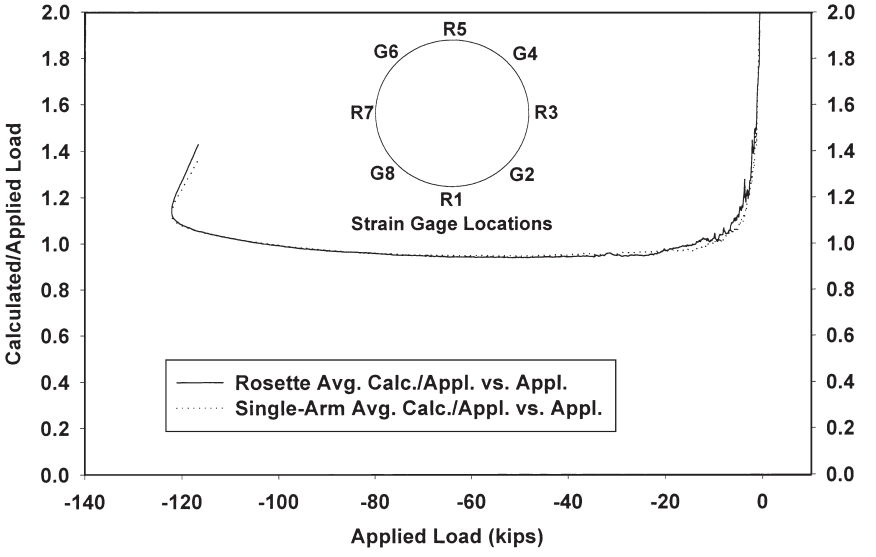

Fig. 7. Comparison of calculated vs. applied load.

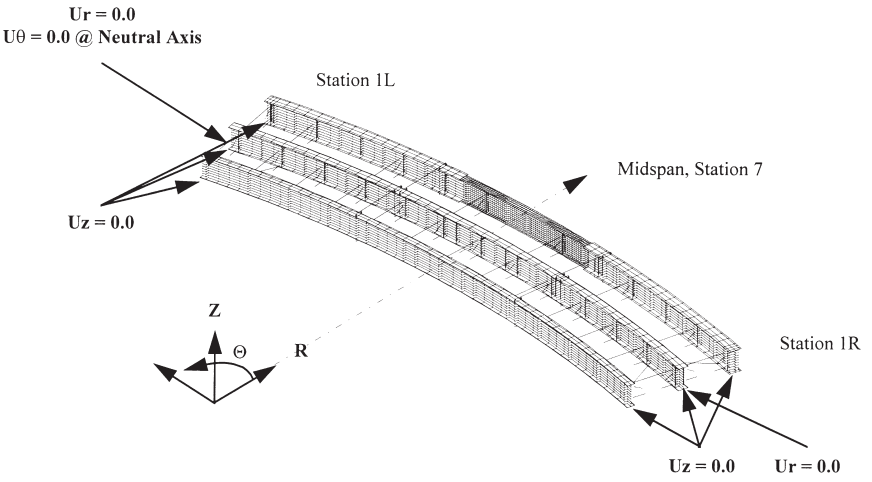

Fig. 8. Coordinate system and boundary conditions.

until yielding was first observed. Once yielding began to propagate through the tube section at mid-height, load was incrementally applied until appreciable plastification of the section, signified by a plateau of the load–strain curve, was obtained. Then, the specimen was unloaded to near original conditions using the same loading rate.

After completing the initial loading cycle, specimens 2C, 3C, 6C, and 1T went through two additional testing cycles. These additional tests were used to validate repeatability of the linear response of the specimens and to observe their post-yield capacity. During each of the two cycles, specimens were reloaded until appreciable plastification was again observed and then the specimens were unloaded to the starting point. Specimen 1C, used to establish a benchmark cross frame specimen capacity, as stated earlier, went through one loading and unloading cycle before being terminated.

Fig. 6 shows the results of one of the concentric compression tests conducted on pipes simulating the top

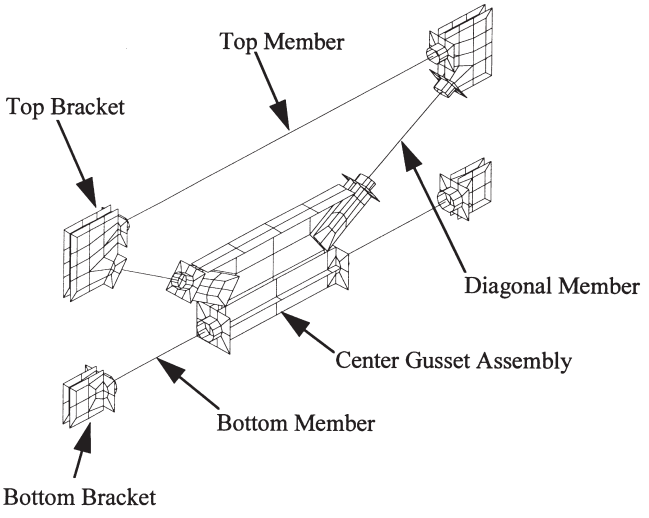

Fig. 9. Cross-frame components.

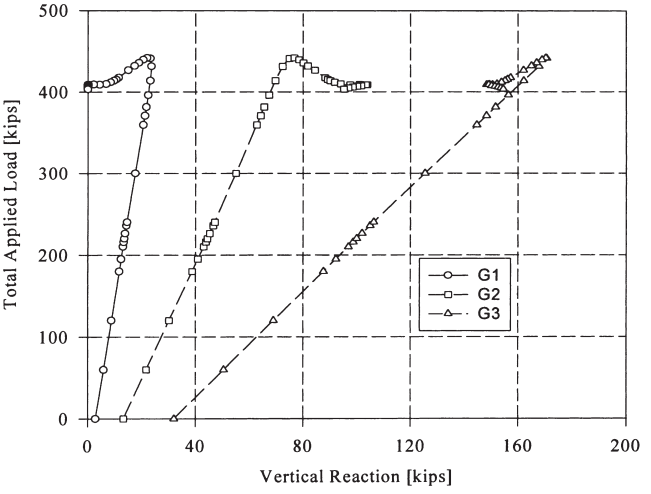

Fig. 10. Reactions at left support versus total applied load for specimen B6.

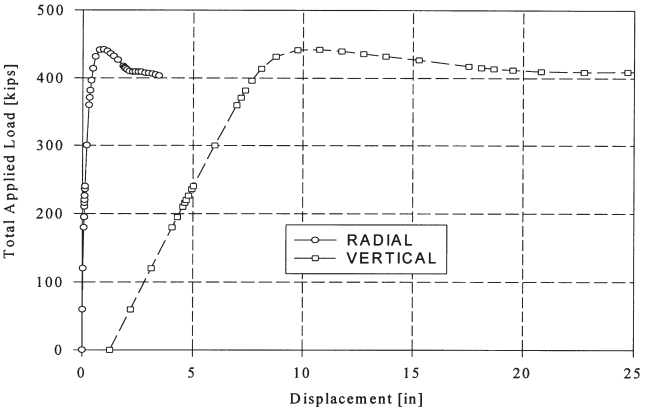

Fig. 11. Radial and vertical displacements for the centerline of specimen B6.

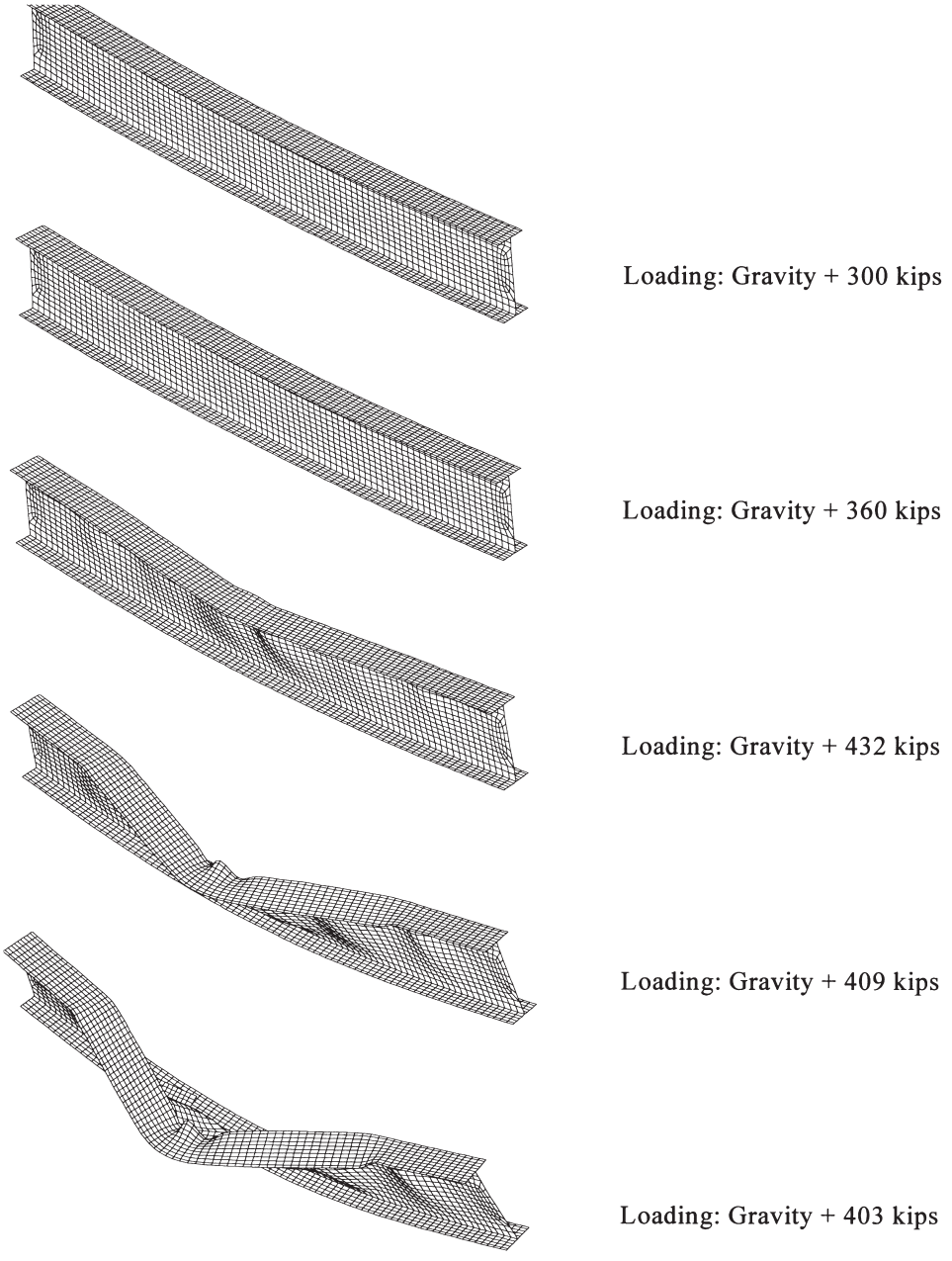

Fig. 12. Progressive deformation of specimen B6 as a function of total applied load.

cross-frame member. The plot shows strains measured from individual longitudinal strain gages (Gages 2 and 6) and from rosette strain gages (Gages R1-2, R3-2, R5-2, and R7-2). The output of the individual quarter-bridge gages was combined into different full-bridge configurations through the use of a spreadsheet to obtain the total forces [8]. Typical results are shown in Fig. 7, which shows a plot of the calculated vs. applied load for the linear range. Comparison of the result indicates very good agreement once the actual dimensions of the tube are used. Nominal values were used for area of the tube for the data shown in Fig. 7, resulting in a ratio of 0.96 in the linear range rather than the 1.00 desired. Similar results have been obtained for eccentric and tension tests.

6. Analytical studies of the test frame

Figs. 1 and 8 show the typical mesh used during the evaluation of the three-girder test configuration. The model shown was developed using the solid modeling package PATRAN Version 3.0, which was then converted to ABAQUS/Aqua Version 5.5 for the detailed analyses. Fig. 1 shows two general levels of discretization: one for test specimens (B1 through B6) and one

for the support test frame. The latter includes the support girders (G1, G2 and G3), the cross frames, the bottom lateral bracing at the ends, the loading fixtures and the bearings. The tests specimens are bolted into the outside girder of the test frame, indicated as support girder G3, through field splices and are laterally supported by the cross frames at stations 6L and 6R. The test frame consists of several components, which can be further broken down into subcomponents. The major components of the test frame consist of the three support girders G1, G2, and G3, the loading fixture, cross frames, bottom flange bracing system, and the bearings, which are supported by concrete abutments.

The geometry of the three-girder test configuration lends itself naturally to being described within a cylindrical coordinate system with the origin located at the center of curvature of the three concentric girders, as indicated in Fig. 8. Fig. 8 also indicates the boundary conditions used for the analyses: vertical restraints at the six bearing locations, radial restraints applied at both ends of the center support girder G2, and a tangential restraint at the neutral axis of support girder G2 at station 1L. The bearings, spherical and radial, are modeled using unidirectional gap elements with a coulomb friction of 5%, thus making it possible to account for the radial and tangential forces experienced at each of the bearings. The bearings are mounted on to steel abutments, which are assumed to be very stiff and are not specifically included in the model.

Presented in Fig. 9 is the model of a complete cross frame which consists of the pipe section top, diagonal and bottom members, and the connecting brackets and center gusset assembly (see also Fig. 2). The pipe section members are retained in the basic model and are capable of undergoing nonlinear plastic deformations. The brackets and gusset assembly are substructured and are thus restricted to linear elastic behavior. Each bracket and gusset assembly represents a separate superelement within the model; thus each cross frame is made up of five superelements and five beam elements.

The FEM described in the preceding sections is comprised of four different element types, consisting of shell, beam, unidirectional gap, and superelements. The general doubly curved shell element S4R in ABAQUS was selected to represent the girder web, flange and stiffener plates because of its ability to represent either thin or thick shells, finite membrane strains, and large rotations.

Fig. 10, Fig. 11 and Fig. 12 show some typical results for specimen B6. Shown in Fig. 10 are the vertical reactions at one end of the bridge versus the total imposed load. This graph shows that the behavior is entirely linear up to a load of 360 kips where the compression flange begins to deform. It also shows that the exterior girder (G3) takes most of the load, and that the interior girder contributes relatively little to the strength of the system for *this* loading condition only. This is true even though a substantial number of stiff cross-frames exists between G1 and G2. Fig. 11 shows the vertical displacements of the compression flange at the centerline of G3. The vertical displacements at maximum strength are appreciable (10 in.), but the strength drops gradually and by less than 10% as the buckling begins. Fig. 12 shows the progression of failure in a highly distorted fashion. The symmetrical shapes shown in Fig. 12 arise because no eccentricities or out-of-straightness effects were incorporated into these analyses.

Acknowledgements

This work was supported by HDR Engineering through the Federal Highway Administration under Contract No. DTFH61-92-C-00136. Sheila Duwadi serves as the Contracting Officer's Technical Representative for the FHWA. The technical input of Dann Hall of Bridge Software Development International, Ltd., and Mike Grubb and John Yadlosky of HDR Engineering, Inc., has been invaluable to this investigation. We also acknowledge the assistance of W. Wright at the Turner-Fairbank Highway Research Center for his assistance in the experimental set up of the full-scale investigation. The results presented herein represent the views and opinions of the authors and not those of the sponsors.

References

[1] AASHO-ASCE Committee on Flexural Members. Survey of curved girder bridges. American Society of Civil Engineers 1973;43(2):54–6.
[2] American Association of State Highway and Transportation Officials. Guide specifications for horizontally curved highway bridges. Washington, DC:AASHTO, 1980.
[3] American Association of State Highway and Transportation Officials. Guide specifications for horizontally curved highway bridges, 1980: as revised by interim specifications for 1981, 1982, 1984, 1985, 1986. Washington DC: AASHTO, 1987.
[4] American Association of State Highway and Transportation Officials. Guide specifications for horizontally curved highway bridges. Washington, DC: AASHTO, 1993.
[5] ASCE-AASHTO Task Committee on Curved Girders. Curved I-girder bridge design recommendations. J Struct Div, ASCE 1977;103(ST5):1137–67.
[6] ASCE-AASHTO Task Committee on Curved Girders. Curved steel box-girder bridges: a survey. J Struct Div, ASCE 1978;104(ST11):1697.
[7] ASCE-AASHTO Task Committee on Curved Girders. Curved steel box-girder bridges: state-of-the-art. J Struct Div, ASCE 1978;104(ST11):1719–39.
[8] Dally JW, Riley WF, McConnell KG. Instrumentation for engineering measurements. New York: Wiley, 1993:584.
[9] De Saint-Venant B. Mémoire sur le calcul de la résistance et de la flexion des pièces solides à simple ou à double courbure, en prenant simultanément en consideration les divers efforts auquels elles puevent êntre soumise dans touts les sens. CR Acad Sci Paris 1843;XVII(942):1020–31.
[10] Galambos TV. Tentative load factor design criteria for curved

steel bridges. Research Report No. 50, School of Engineering and Applied Science, Civil Engineering Department, Washington University, St. Louis, May 1978.

[11] Galambos TV, Hajjar JF, Leon RT, Huang WH, Pulver B, Pulver Rudie. Stresses in steel curved girder bridges. Report Number 96-28, University of Minnesota, Center for Transportation Studies, 1996.

[12] Ketchek KF. Discussion of "Horizontally curved birders—state of the art" by McManus PF et al. J Struct Div, ASCE 1969;95(ST12):2999–3001.

[13] McManus PF, Nasir GA, Culver CG. Horizontally curved girders—state of the art. J Struct Div, ASCE 1969;95(ST5):853–70.

[14] Nakai H, Yoo CH. Analysis and design of curved steel bridges. New York: McGraw-Hill, 1988:768.

[15] Pandit GS, Ceradini G, Garvarini P, Eremin AA. Discussion of "Horizontally curved girders—state of the art". J Struct Div, ASCE 1970;96(ST2):433–6.

[16] Stegmann TH, Galambos TV. Load factor design criteria for curved steel girders of open section. Research Report 23, Civil Engineering Department, Washington University, St. Louis, April 1976.

[17] Tan CP, Shore S, Ketchek K. Discussion of "Horizontally curved girders—state of the art" by McManus PF et al. J Struct Div, ASCE 1969;95(ST12):2997–9.

[18] Zureick A, Naqib R, Yadlosky J. Curved steel bridge research project, interim report I: synthesis. Report No. FHWA-RD-93-129, Federal Highway Administration, December 1994.